American Journal of Botany and Bioengineering
https://biojournals.us/index.php/AJBP
ISSN: 2997-9331

Study the Mechanism of Color Depigmentation by Q-Switched Nd-Yag Laser Photoacoustic Shouckwave

Alaa Hashim Salman Abass
University of Technology Department Laser and optoelectronics engineering

Ahmed Haitham Mahidi Saleh
Anbar University College of Science Department of Physics

Received: 2024 19, Sep
Accepted: 2024 28, Sep
Published: 2024 18, Oct

Annotation: The proportion of children with chronic adenotonsillitis varies from 20 to 50 per cent, and 37 to 70 per cent of frequently ill children. This indicates an increase in pharyngeal tonsil hypertrophy, an increase in the incidence of adenoid pathology in children, which adversely affects the structural formation of the jaw complex. It has been revealed that the influence of the long-term course of diseases in children leads to a violation of the formation of the facial skeleton, which is reflected in the form of a sagging lower jaw, its narrowing and distant, improper development of the hard palate and occlusion. In the development of dentoalveolar anomalies at the age of 8-10 years, diseases of the ENT organs, in particular, overgrowth of adenoids, play a significant role.

Keywords: Anthropometry, adenoidectomy, adenoid hypertrophy, children

1.1. Introduction

Breast cancer (BC) is a prevalent malignant neoplasm and ranks as the second most prevalent cancer among women (DeSantis, Carol E., et al. 2019) . Around 1.5 million new instances of breast cancer are diagnosed each year (Reje , et .al ,2024) and almost 460,000 women succumb to the disease yearly as a result of BC chemoresistance and metastasis. The biological features of breast cancer (BC) are often used for early identification, prognosis, and the determination of an appropriate treatment approach. These characteristics include histologic subtype, grade (Han, et , al 2020) lymph node status, hormone receptor, and human epidermal growth factor receptor 2 (HER2) statuses (Behairy , et. al . 2022) The above qualities are associated with patients' survival and clinical outcomes after therapy (Sparano, Joseph A., et al. 2020).

Nevertheless, several breast cancer patients, exhibiting comparable features had varying clinical outcomes. Hence, the diagnostic, prognostic, and clinical outcome prediction of biological characteristics are subject to some limitations (Turkki, Riku, et al. 2019). Therefore, there is an urgent need for breakthrough diagnostic and prognostic methodologies to identify categorizing therapy options that may enhance the quality of life for patients with breast cancer.

Mature microRNAs (miRNAs) are a class of tiny RNA molecules composed of around 19-25 nucleotides. These molecules are crucial in several biological processes, such as cell differentiation, cell proliferation, apoptosis, and stress response (Annese, Tiziana, et al. 2020 , Hussen, et ,al 2021) . The post-transcriptional mechanism is the primary process via which miRNAs modulate gene expression. This mechanism involves binding miRNAs to the 3' untranslated region (UTR) of mRNAs, destroying them. The eight-base seed region of the miRNA is the primary factor influencing this process, since it is the area of the miRNA that exhibits the highest degree of complementarity to the target mRNA. Upon binding to the 3’ UTR, the miRNA attracts proteins that break down the mRNA (Li, Lu, et al.2021, Shafabakhsh, Rana, et al.2019) . Furthermore, authors have reported the existence of additional regulatory mechanisms, including the elimination of polyadenine chains from the mRNA (Abadi ,et , al 2019) and the control of translation initiation by binding to specific locations within the coding region of mRNAs (Roos, Dirk et ,al 2021). Therefore, by establishing an intricate network between miRNA and mRNA, a solitary miRNA can directly or indirectly target many mRNAs, therefore coordinating multiple biological activities simultaneously (Wu , et ,al 2023) . It has been reported that each miRNA may categorize around 100-200 target sites throughout the transcriptome.

2.1 Overview

Ten-millilitre test tubes, specifically designed to separate serum, collected blood samples. The total number of serum samples collected was thirty, with ten samples coming from healthy women who volunteered their time and twenty samples coming from women who had been diagnosed with breast cancer. After being left for a half an hour, the blood was centrifuged for five minutes at a speed of 1600 revolutions per minute. After transferring the serum into 2ml Eppendorf tubes, it was kept at -20 degrees Celsius for further analysis. These samples were collected from women who were recipients of treatment at the Breast Cancer Unite at Al-Karama Teaching Hospital in Baghdad. The system (3-1) was used to determine the progress of the current research stages.

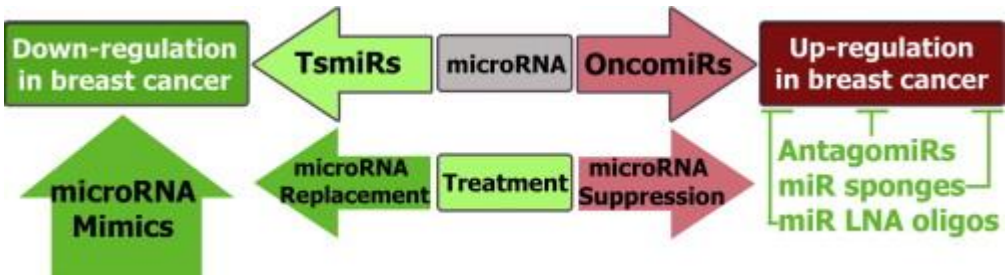

Figure 2. 1 Steps of the research project

2.2 MicroRNA extraction from serum and plasma Samples

The extraction of miRNA from serum samples was performed using a plasma/serum circulating RNA purification kit in slurry format, following the prescribed technique.

1. A combination of two solutions (1.8 ml of lysis buffer solution B and 0.2 ml of solution A) was added to 1 ml of serum or plasma. The mixture was vortexed for 15 seconds and then incubated at 60°C for 10 minutes.
2. Following the incubation period, 3ml of pure ethanol was introduced. Agitated via vortexing for 15 seconds and subjected to centrifugation at 1000 X g for 30 seconds.
3. The supernatant was meticulously separated, adding 0.3 ml of solution C to the slurry pellet. The samples were then combined by vortexing for 15 seconds and incubated at 60 °C for 10 minutes.
4. Following the incubation period, 0.3 ml of pure ethanol was introduced and agitated by vortexing for 15 seconds. Subsequently, the mixture was transferred to a microfilter spin column and centrifuged for 1 minute at a force of 14000 X g. The flow-through was subsequently disposed of.
6. A 0.4 ml aliquot of washing solution was introduced into the column and subjected to centrifugation for 1 minute at a force of 14000 X g. The fluid flow was disposed of. The procedure mentioned above was iterated thrice.
7. The vacant column underwent centrifugation for 3 minutes at a force of 14000 X g, after which the collecting tube was disposed of.
8. The spin column was moved to a new 1.7 ml elution tube, and 100 µl of elution solution was added. The column was then centrifuged at 2000 X g for 2 minutes, followed by centrifugation at 14000 X g for 3 minutes.
9. The solution containing free circulation RNA was held at -80ºC until ready.

2.2.1 Kits

Table 2.1 Component of kit

Kits	Company/ Origin
Chloroform	Alpha Chemika, INDIA
EntiLink™ Reverse Transcriptase	ELK Biotechnology, Chine
EnTurbo™ SYBR Green PCR SuperMix	ELK Biotechnology, Chine
Isopropanol, 70% Ethanol	Alpha Chemika, INDIA
Primers	Macrogen, Korea
TRIzol Reagent	ELK Biotechnology, Chine
Quantifluor dsDNA System	Promega, USA

2.3 Primers

Table 2.2 Components of Primers

Primer Name	Seq.
miR-425 RT-primer	GTTGGCTCTGGTGCAGGGTCCGAGGTATTCGCACCAGAGCCAACTCAACG
miR-425 F	GGTTTTTTTTAGCAGCACGTAAAT
Universal Reverse	GTGCAGGGTCCGAGGT

miR-16-1 RT-primer	GTTGGCTCTGGTGCAGGGTCCGAGGTATTCGCACCAGAGCCAACCGCCAAT
miR-16-F	GGTTTTTTTTAGCAGCACGTAAAT

2.4 Instrument

Table 2.3 Tools and equipments

Instrument	Company/ Origin
1.5ml, 0.5ml and 0.2ml Tube	JET BIOFIL, Singapore
Centrifuge	Phenox, China
SimpliAmp Thermal Cycler	Applied Biosystem, USA
Micropipette	Human, Germany
Quantus Fluorometer	Promega, USA
Refrigerator	TEKA, Spain
Vortex	ISOLAB, China
Water bath	China

2.5 Methods and Workflow

RNA Purification

RNA was isolated from the sample according to the protocol of TRIzol™ Reagent as the following steps:

A. Sample lysis

Serum sample

For each tube, 0.4 mL of serum was added to 0.5 mL of TRIzol™ Reagent, and the lysate was homogenized by pipetting up and down several times.

B. For the three phase's separation

- 0.2 mL of chloroform was added to the lysate for each tube, and then the tube cap was secured.
- All mixes were Incubated for 2–3 minutes and then centrifuged for 10 minutes at 10,000 rpm. The mixture was separated into a lower organic phase, interphase, and a colourless upper aqueous phase.
- The aqueous phase containing the RNA was transferred to a new tube.

C. For RNA precipitation

- 0.5 mL of isopropanol was added to the aqueous phase, incubated for 10 minutes, and then centrifuged for 10 minutes at 12,000 rpm.
- Total RNA was precipitated, and a white gel-like pellet was formed at the bottom of the tube.
- The supernatant was then discarded.

D. For RNA washing

- For each tube, 0.5mL of 70% ethanol was added and vortexed briefly, then centrifuged for 5 minutes at 10000 rpm.
- Ethanol was then aspirated and air-dried in the pellet.

E. For RNA solubility

- The pellet was rehydrated in 50µl of Nuclease Free Water, then incubated in a water bath or heat block set at 55–60°C for 10–15 minutes.

3. Results and Discussion

3.1 Dataset

From December 3, 2023, to March 12, 2024, blood samples were collected from twenty women who had been diagnosed with breast cancer and ten healthy women who represented the control group. The samples were collected with the assistance of the Al-Fallujah teaching hospital in (Al Anbar, Iraq) . The findings shown in Table (3.1) indicate that the ages of the women who were diagnosed with breast cancer varied from 22 to 70 years, with the average age of breast cancer patients reaching 47.5 years. Conversely, the typical age of women experiencing good health was 39 years.

Table 3. 1 Dataset of the participants

Case	Sample	Age (year)	BIRADS * Result
1	Cancer	63	4
2	Cancer	64	5
3	Cancer	42	5
4	Cancer	40	5
5	Cancer	40	4
6	Cancer	22	None
7	Cancer	50	4
8	Cancer	56	Metastasis
9	Cancer	63	Ductal Carcinoma
10	Cancer	47	4
11	Cancer	50	3
12	Cancer	36	4
13	Cancer	45	4
14	Cancer	50	4
15	Cancer	50	3
16	Cancer	46	5
17	Cancer	36	Metastasis
18	Cancer	50	4
19	Cancer	70	6
20	Cancer	30	4
21	Healthy	54	1
22	Healthy	41	1
23	Healthy	31	2
24	Healthy	33	1
25	Healthy	50	2
26	Healthy	35	2
27	Healthy	30	0
28	Healthy	46	1
29	Healthy	40	Zero
30	Healthy	30	1

*The acronym BIRADS stands for Breast Imaging-Reporting and Data System. The BI-RADS Assessment Categories consist of the following: 0 represents Incomplete, 1 represents Negative, 2 represents Benign finding(s), 3 represents Probably benign, 4 represent Suspicious abnormality, 5

represent Highly suggestive of malignancy, and 6 represent Known biopsy – proved malignancy [83].

3.2 Protocol (mic-16)

Volume(1-125ul): 20

Lid work status: ON

Lid Temp.(100-105°C): 105

Table 3. 2 Scanning the position for miRNA-16

	One	Two	Three	Four	Five	Six
Scan Positions:	ON	ON	ON	ON	ON	ON
	CH1	CH2	CH3	CH4	CH5	CH6
Scan Channels:	ON	OFF	OFF	OFF	OFF	OFF

Steps

When referring to mic-16, the term "protocol" denotes a predetermined sequence of actions or directives that must be adhered to to conduct a particular experiment or assignment. The experimental procedure entails the manipulation of liquid volumes, which span a range of 1 to 125 microliters. This is carried out in a regulated environment, with the lid in a functional position and the temperature between 100 and 105°C. The methodology comprises a series of consecutive temperature cycles: an initial preheating phase of 180 seconds at 95°C, succeeded by subsequent cycles of 20 seconds at 95°C, 20 seconds at 59°C, and 20 seconds at 72°C. The cycle above is iterated 46 times before entering an indefinite cooldown phase at 0°C, after which the protocol loops to its inception.

1: 95°C for 180S;
2: 95°C for 20S;
3: 59°C for 20S;
4: 72°C for 20S;
5: GOTO 2, 45 more times;
6: 0°C for 0S;
7: 0°C for 0S;
8: GOTO 0, 65536 more times;

Plate Layout

The Plate Layout, as illustrated in Figure (4.1), is a graphical representation showcasing the spatial organisation of various components, including controls, samples, and well plates, utilised in the miRNA-16 analysis. Ensuring the correct positioning of experimental components, adherence to experimental design, and consistency in experimental outcomes are all contingent upon this layout. It functions as an indispensable reference instrument for researchers, offering unambiguous visual direction during the implementation of the mic-16 protocol.

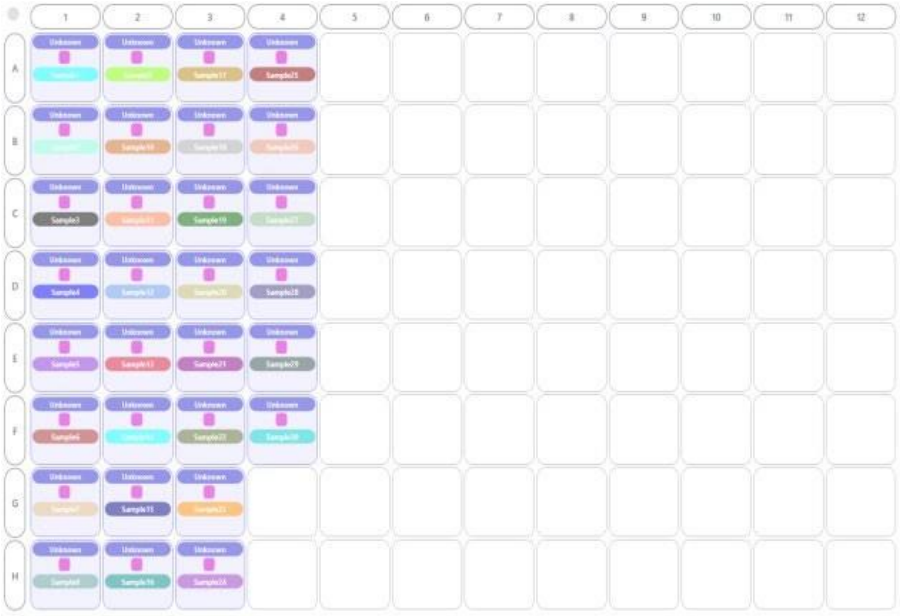

Figure 3.1 Plate layout for miRNA-16

Quantification

Amplification Chart

Analysis Settings Type: Linear

Colour by: Sample

The term "Amplification Chart" denotes a visual depiction that shows the dynamic amplification of miRNA-16 throughout the experimental protocol. The parameter "Analysis Settings Type" determines the approach utilised to analyse the data; in this case, "Linear" signifies implementing a linear regression analysis methodology. Furthermore, the inclusion of the "Colour by: Sample" option implies that the amplification chart's data points or curves are visually distinguished and depicted by the particular sample to which they pertain. The visual representation of the amplification process, known as the Amplification Chart for miRNA-16 (Figure 4.2), is presumed to assist scientists in interpreting and analysing the experimental outcomes acquired via the mic-16 protocol.

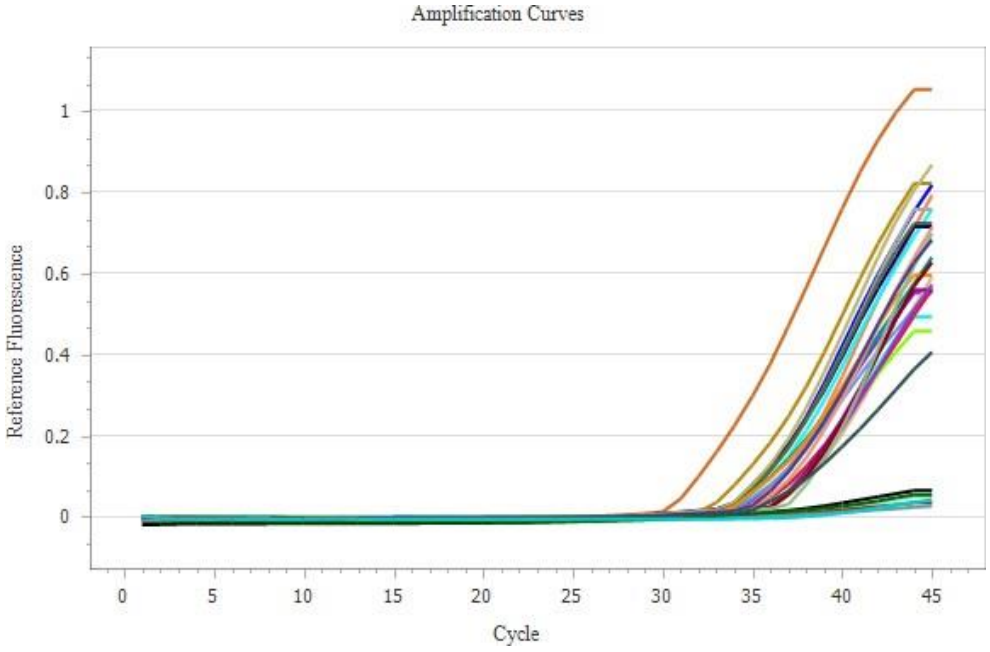

Figure 3. 2 Amplification Chart for miRNA-16

Melting Curve Chart

Analysis Settings

Type: Derivative

Color by: Sample

In the "Analysis Settings" section, the parameters utilised to analyse the data obtained from the melting curve are specified. The utilisation of the "Type: Derivative" parameter in this case indicates that the analysis is predicated on the melting curve's derivative. This likely aids in the detection of unique melting peaks or transitions that are linked to miRNA-16. In addition, the parameter labelled "Colour by: Sample" specifies that data points or curves depicted on the melting curve chart are color-coded by the particular sample they symbolise. This feature facilitates the distinction and analysis of findings. The Melting Curve Chart for miRNA-16 (2), depicted in Figure (4.4), offers researchers a graphical representation of the melting characteristics miRNA-16 under various experimental circumstances. This visual aid aids in interpreting and analysing the data produced by the mic-16 protocol.

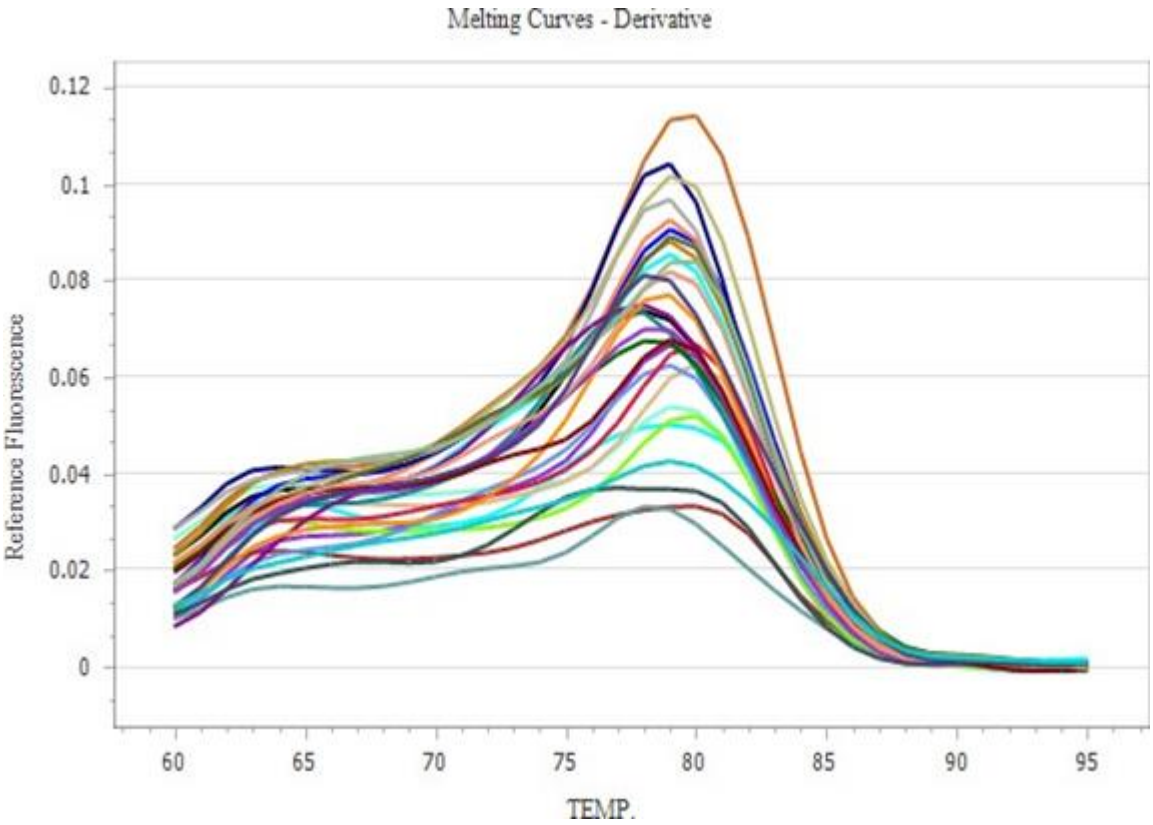

Figure 3.4 Melting Curve Chart for miRNA-16(2)

Quality Control

Table 4.3, entitled "Quality Control for miRNA-16," provides an overview of different quality control measures and their respective frequencies, locations, and descriptions within the experimental configuration. Criteria for these assessments comprise positive controls with cycle threshold (Cq) values exceeding zero, non-template controls (NTCs) with Cq values below zero, and negative controls with Cq values below zero. Additionally, the frequency and location of specific events, including standard samples lacking Cq values and unknown samples lacking Cq values, are detailed in the table for each well in the experimental configuration. By implementing these quality control measures, scientists can bolster the dependability of their experimental findings by guaranteeing the precision, reproducibility, and validity of the data acquired via the mic-16 protocol.

Table 3. 3 Quality Control for miRNA-16

Flag	Description	Frequency	Wells
Negative Control Less	Negative control with a Cq less than	0	
NTC Less	NTC with a Cq less than	0	
NRT Less	NRT with a Cq less than	0	
Positive Control Greater	Positive control with a Cq greater than	0	
Unknown Without Cq	Unknown without a Cq	6	B1,C1,F1,H1,C3,F4,
Standard Without Cq	Standard without a Cq	0	
Efficiency Greater	Efficiency greater than	0	
Efficiency Less	Efficiency less than	24	A1,D1,E1,G1,A2,B2,C2,D2,E2,F2,G2,H2 ,A3,B3,D3,E3,F3,G3,H3,A4,B4,C4,D4,E4
StdCurveR2Less	Std Curve R^2 less than	0	
Replicate Group Std Dev Greater	Replicate group Cq Std Dev greater than	0	

Analysis Results

The results are detailed on various parameters associated with each analysed sample and are presented in Table (4.4). The table presents distinct wells in the experimental configuration, each accompanied by relevant data, including the name of the sample, the target channel, the fluorescence type, the function, the cycle threshold (Cq), the mean Cq, the Cq standard deviation (CqStd), the quantification, the melting temperature (Tm), and the relative fluorescent units (RFU). Significantly, the Cq value signifies the cycle of mass detection, whereas CqStd denotes the deviation from the mean of the fundamental Cq values. Furthermore, the temperature at which molecules undergo melting is denoted as Tm, while the intensity of quenching utilised in detection operations is quantified in RFU. The outcomes of this analysis are of the utmost importance in assessing the effectiveness and efficiency of the mic-16 protocol. They enable the interpretation and validation of experimental discoveries associated with miRNA-16 analysis.

Table 3. 4 Analysis Results for miRNA-16

Well	Sample	Target	Fluorescence	Function	Cq	CqMean	CqStd	Quantity	Tm	RFU
A1	Sample 1	Channel1	FAM	UNKNOWN	34.417	34.417	0	0	79.16	4933
B1	Sample 2	Channel1	FAM	UNKNOWN	NaN	NaN	NaN	0	79.594	503
C1	Sample 3	Channel1	FAM	UNKNOWN	35.664	35.664	0		78.354	651
D1	Sample 4	Channel1	FAM	UNKNOWN	34.717	34.717	0	0	79.436	8170
E1	Sample 5	Channel1	FAM	UNKNOWN	34.934	34.934	0	0	79.386	5512
F1	Sample 6	Channel1	FAM	UNKNOWN	NaN	NaN	NaN	0	79.521	348
G1	Sample 7	Channel1	FAM	UNKNOWN	36.521	36.521	0	0	80.223	5915
H1	Sample 8	Channel1	FAM	UNKNOWN	41.649	41.649	0	0	78.712	271
A2	Sample 9	Channel1	FAM	UNKNOWN	NaN	NaN	NaN	0	79.978	4573
B2	Sample 10	Channel1	FAM	UNKNOWN	30.796	30.796	0	0	79.972	10519
C2	Sample 11	Channel1	FAM	UNKNOWN	35.445	35.445	0	0	79.332	7922
D2	Sample 12	Channel1	FAM	UNKNOWN	34.386	34.386	0	0	79.179	5569
E2	Sample 13	Channel1	FAM	UNKNOWN	35.459	35.459	0	0	80.063	5604
F2	Sample 14	Channel1	FAM	UNKNOWN	34.895	34.895	0	0	79.254	7578
G2	Sample 15	Channel1	FAM	UNKNOWN	34.553	34.553	0	0	79.131	7150
Well	Sample	Target	Fluorescence	Function	Cq	CqMean	CqStd	Quantity	Tm	RFU
H2	Sample 16	Channel1	FAM	UNKNOWN	34.429	34.429	0	0	78.005	6394
A3	Sample 17	Channel1	FAM	UNKNOWN	33.489	33.489	0	0	79.344	8211
B3	Sample 18	Channel1	FAM	UNKNOWN	34.842	34.842	0	0	79.158	7572
C3	Sample 19	Channel1	FAM	UNKNOWN	NaN	NaN	NaN	0	78.523	549
D3	Sample 20	Channel1	FAM	UNKNOWN	34.61	34.61	0	0	79.478	8669
E3	Sample 21	Channel1	FAM	UNKNOWN	36.387	36.387	0	0	78.037	5587
F3	Sample 22	Channel1	FAM	UNKNOWN	34.672	34.672	0	0	79.421	7228
G3	Sample 23	Channel1	FAM	UNKNOWN	34.753	34.753	0	0	79.089	5948
H3	Sample 24	Channel1	FAM	UNKNOWN	36.324	36.324	0	0	78.626	5714
A4	Sample 25	Channel1	FAM	UNKNOWN	36.583	36.583	0	0	79.376	6269

B4	Sample 26	Channel1	FAM	UNKNOWN	36.089	36.089	0	0	79.354	7125
C4	Sample 27	Channel1	FAM	UNKNOWN	37.07	37.07	0	0	79.705	6979
D4	Sample 28	Channel1	FAM	UNKNOWN	35.334	35.334	0	0	78.753	6821
E4	Sample 29	Channel1	FAM	UNKNOWN	NaN	NaN	NaN	0	78.426	4058
F4	Sample 30	Channel1	FAM	UNKNOWN	NaN	NaN	NaN	0	79.303	423

*Cq: means cycle threshold, which is the cycle at which mass detection occurs.

*CqStd: means the cycle standard deviation threshold and is a standard deviation of the fundamental Cq values.

*Tm means melting temperature, which is the temperature at which molecules are melted.

*RFU means relative fluorescent units, a unit of measurement for the intensity of quenching used in detection operations.

3.3 Protocol Micro 425

Volume(1-125ul): 20

Lid work status: ON

Lid Temp.(100-105°C): 105

Table 3. 5 Scanning the positivon for miRNA-425

	One	Two	Three	Four	Five	Six
Scan Positions:	ON	ON	ON	ON	ON	ON
	CH1	CH2	CH3	CH4	CH5	CH6
Scan Channels:	ON	OFF	OFF	OFF	OFF	OFF

Steps

Within the framework of Protocol Micro 425, the protocol describes a sequence of procedures that must be followed to carry out a particular scientific experiment or activity. The protocol calls for manipulating liquid volumes ranging from one microliter to one hundred and twenty-five microliters inside an environment where the lid operates, and the temperature is maintained between one hundred and ten degrees Celsius. The procedure, beginning with step 1 (cycle), should be repeated 65536 more times. These steps probably aim to make a particular experimental procedure easier to carry out, such as the polymerase chain reaction (PCR) or other temperature-dependent reactions. This is accomplished by supplying the precise temperature control and cycling conditions required for amplifying or manipulating genetic material or other biological samples.

1: 95°C for 180S;
2: 95°C for 20S;
3: 59°C for 20S;
4: 72°C for 20S;
5: GOTO 2, 45 more times;
6: 0°C for 0S;
7: 0°C for 0S;
8: GOTO 0, 65536 more times;

Plate Layout

The "Plate Layout" defines the configuration of components such as controls, samples, reagents, or other elements on a tangible plate or well plate utilised in the experiment, as specified in Protocol Micro 425. The layout illustrated in Figure 4.5 is a visual reference that delineates the specific locations of different components essential for the protocol. The precise and consistent execution of the experiment is dependent on the Plate Layout, which delineates the locations of various controls and samples throughout the experimental apparatus. Technicians and researchers utilise this configuration to guarantee that samples are pipetted, mixed, and analysed by the established protocol. The Plate Layout functions as a benchmark instrument, facilitating the replication and dependability of experimental outcomes acquired via Protocol Micro 425, specifically in investigations of the analysis of miRNA-425.

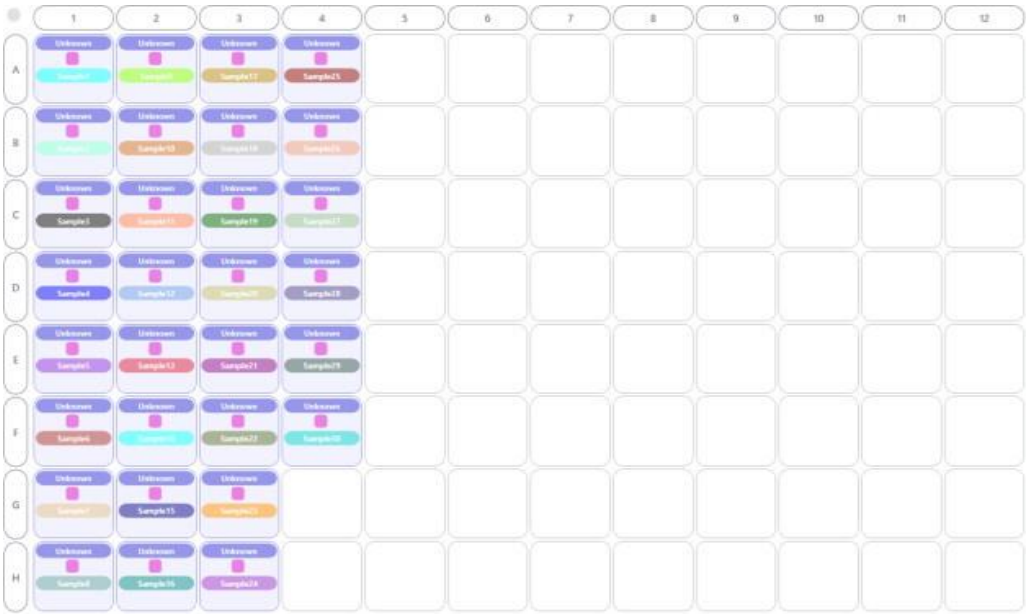

Figure 3.5 Plate Layout for miRNA-425

Quantification

Amplification Chart

Analysis Settings Type: Linear

Colour by: Sample

Amplification Chart

"Quantification" and "Amplification Chart" are essential elements of the experimental procedure as outlined in Protocol Micro 425. Ascertaining the quantity or concentration of a particular substance, which is probable mi-RNA-425, through using a quantitative technique like PCR (polymerase chain reaction), constitutes quantification. An illustration of the amplification dynamics of mi-RNA-425 throughout the PCR procedure is provided in the Amplification Chart (Figure 4.6). The data demonstrates that the fluorescence signal increases with the number of PCR cycles, suggesting that the target mi-RNA-425 is amplified exponentially. The "Linear" option under "Analysis Settings" indicates applying a linear regression analysis method to examine the amplification data. This facilitates the precise determination of the initial quantity of mi-RNA-425 introduced into the samples. Additionally, the "Colour by: Sample" option enables the differentiation of amplification chart data points or curves according to the specific sample. This feature simplifies the process of interpreting and comparing results. In general, the Amplification Chart and its corresponding analysis parameters are of paramount importance when quantifying mi-RNA-425 levels and interpreting outcomes acquired via Protocol Micro 425.

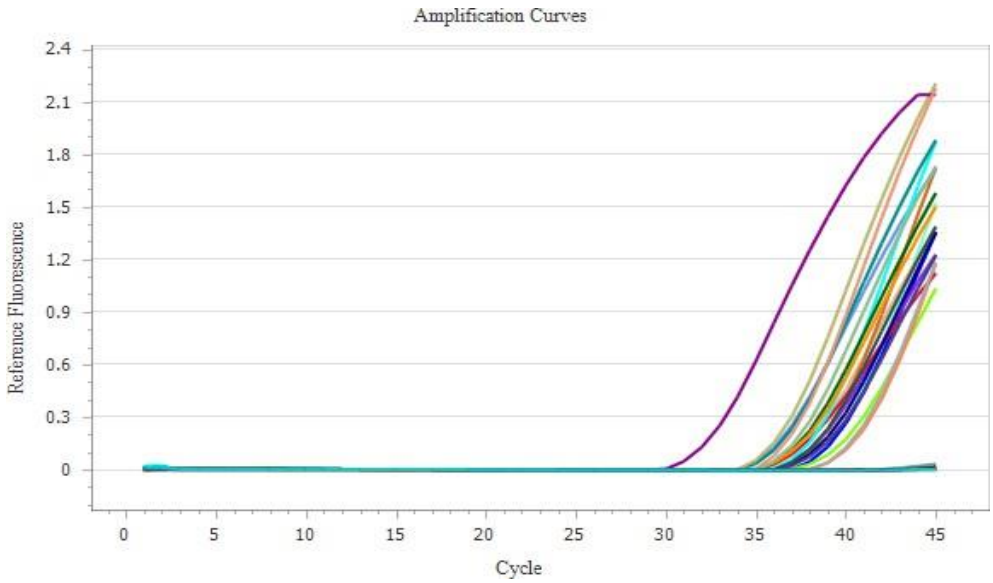

Figure 3. 6 Amplification Chart for mi-RNA-425

Melting Curve Chart

Analysis Settings

Type: Derivative

Color by: Sample

The graphical representation known as the "Melting Curve Chart" in Protocol Micro 425 depicts the controlled melting behaviour of miRNA-425. The chart illustrated in Figure 4.8 offers valuable insights into the dissociation of the amplified miRNA-425 strands to temperature. The method utilised to analyse the melting curve data is specified in the "Analysis Settings." The configuration in this instance is "Type: Derivative," which signifies that the analysis is predicated on the melting curve's derivative. The utilisation of this derivative analysis method facilitates the detection of unique melting peaks or transitions that are linked to miRNA-425. Furthermore, the "Colour by: Sample" option enables the differentiation of melting curve chart data points or curves according to the particular sample to which they pertain. This feature enhances the ability to compare and interpret the melting behaviour of various samples. The insights gained from the Melting Curve Chart and its corresponding analysis parameters regarding the thermal stability and properties of miRNA-425 contribute significantly to comprehending its configuration in relation to Protocol Micro 425.

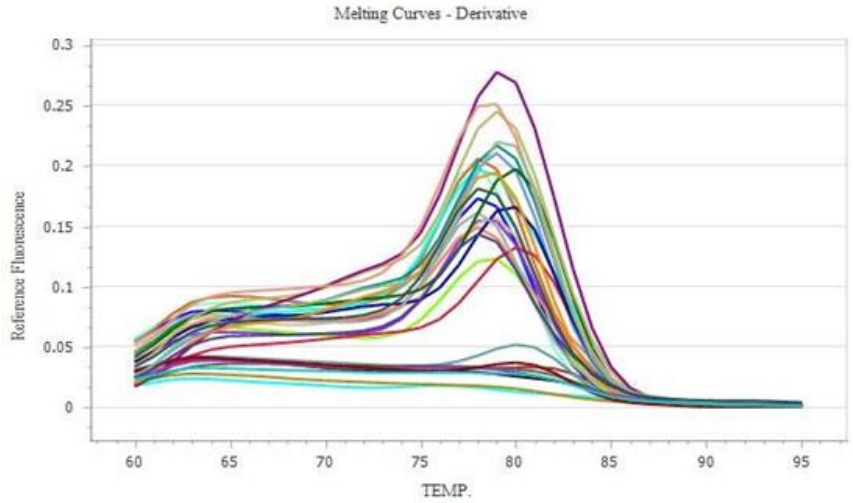

Figure 3. 7 Melting Curve Chart for miRNA-425

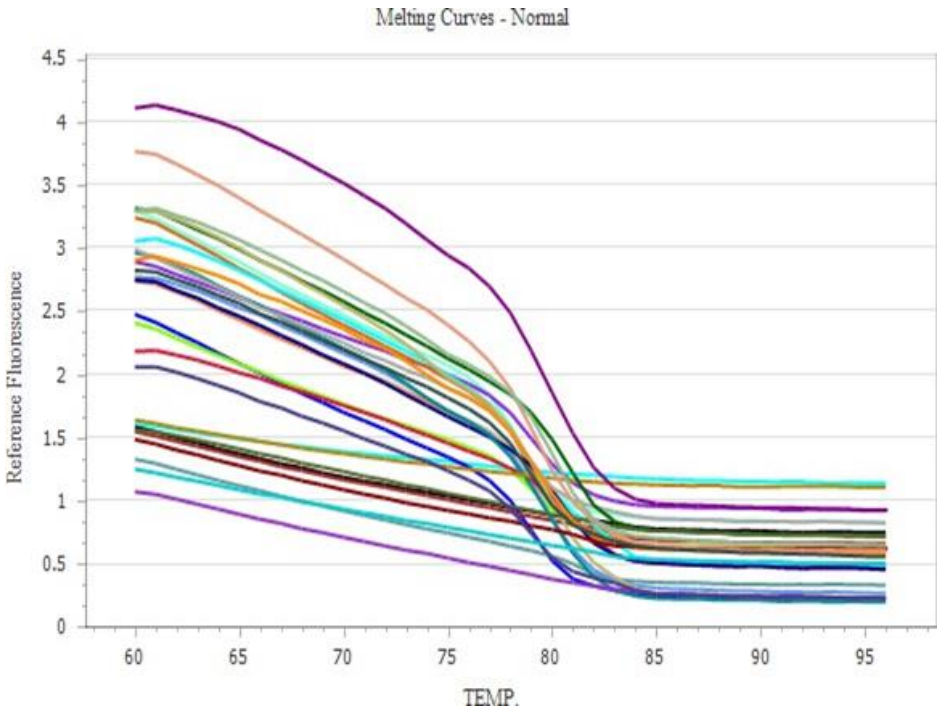

Figure 3. 8 Melting Curve Chart for miRNA-425(2}

Quality Control

Protocol Micro 425 incorporates "Quality Control" measures to guarantee the dependability and precision of experimental outcomes concerning the analysis of miRNA-425. Table (4.6), entitled "Quality Control for miRNA-425," provides a comprehensive overview of the quality control criteria utilised in the experiment, including their descriptions, frequencies, and positions. The criteria encompass the inclusion of positive controls with cycle threshold (Cq) values greater than zero, in addition to negative controls, non-template controls (NTCs), and the absence of reverse transcriptase controls (NRTs) with Cq values below zero. Furthermore, the table delineates instances where unidentified samples lack Cq values, efficiency surpasses or falls short of specific thresholds, and standard curve parameters, including R^2 values below zero. The table provides detailed information regarding the frequency and location of these occurrences within the wells of the experimental configuration. Through strict adherence to these quality control measures, scientists can bolster the dependability of their experimental discoveries of miRNA-425 analysis by guaranteeing the authenticity and uniformity of the data acquired via Protocol MicroRNA- 425.

Table 3. 6 Quality Control for miRNA-425

Flag	Description	Frequency	Wells
Negative Control Less	Negative control with a Cq less than	0	
NTC Less	NTC with a Cq less than	0	
NRT Less	NRT with a Cq less than	0	
Positive Control Greater	Positive control with a Cq greater than	0	
Unknown Without Cq	Unknown without a Cq	9	A1,C1,F1,H1,A3,F3,H3,A4,F4,
Standard Without Cq	Standard without a Cq	0	

Efficiency Greater	Efficiency greater than	0	
Efficiency Less	Efficiency less than	21	B1,D1,E1,G1,A2,B2,C2,D2,E2,F2,G2,H2, B3,C3,D3,E3,G3,B4,C4,D4,E4,
StdCurveR2Less	Std Curve R^2 less than	0	
Replicate Group Std Dev Greater	Replicate group Cq Std Dev greater than	0	

Analysis Results

"Analysis Results" in Protocol Micro 425 contains comprehensive information concerning examining miRNA-425 samples. The results of the analyses for miRNA-425 are detailed in Table 4.7, which includes information on a range of parameters associated with each analysed sample. Every individual row in the table corresponds to a distinct well in the experimental configuration, accompanied by pertinent information including the name of the sample, the target channel, the type and function of fluorescence, the cycle threshold (Cq), the mean Cq, the Cq standard deviation (CqStd), the quantification, the melting temperature (Tm), and the relative fluorescent units (RFU). These parameters provide valuable information regarding the characteristics and efficacy of the miRNA-425 samples being examined. As an illustration, the symbol Cq denotes the cycle of mass detection, whereas CqStd signifies the standard deviation of the fundamental Cq values. Furthermore, the temperature at which molecules undergo melting is denoted as Tm, while the intensity of quenching utilised in detection operations is quantified in RFU. The information in Table 4.7 is of utmost importance in assessing the outcomes achieved via Protocol Micro 425, as it facilitates the interpretation and comprehension of the results of the miRNA-425 analysis.

Table 3. 7 Analysis Results for miRNA-425

Well	Sample	Target	Fluorescence	Function	Cq	CqMean	CqStd	Quantity	Tm	RFU
A1	Sample 1	Channel1	FAM	UNKNOWN	36.440	36.440	0	0	64.059	-14
B1	Sample 2	Channel1	FAM	UNKNOWN	36.58	36.58	0	0	78.177	15185
C1	Sample 3	Channel1	FAM	UNKNOWN	42.828	42.828	0	0	64.296	32
D1	Sample 4	Channel1	FAM	UNKNOWN	37.054	37.054	0	0	78.527	13507
E1	Sample 5	Channel1	FAM	UNKNOWN	39.841	39.841	0	0	78.796	12258
F1	Sample 6	Channel1	FAM	UNKNOWN	42.1	42.1	0	0	64.928	193
G1	Sample 7	Channel1	FAM	UNKNOWN	35.095	35.094	0	0	79.089	13836
H1	Sample 8	Channel1	FAM	UNKNOWN	41.461	41.461	0	0	80.204	329
A2	Sample 9	Channel1	FAM	UNKNOWN	38.638	38.638	0	0	79.066	10335
B2	Sample 10	Channel1	FAM	UNKNOWN	36.068	36.068	0	0	78.534	17198
C2	Sample 11	Channel1	FAM	UNKNOWN	37.892	37.892	0	0	78.427	11767
D2	Sample 12	Channel1	FAM	UNKNOWN	33.651	33.651	0	0	79.317	17133

E2	Sample 13	Channel1	FAM	UNKNOWN	35.08	35.08	0	0	80.375	11195
F2	Sample 14	Channel1	FAM	UNKNOWN	35.516	35.516	0	0	78.746	18705
G2	Sample 15	Channel1	FAM	UNKNOWN	36.086	36.086	0	0	79.994	13554
Well	Sample	Target	Fluorescence	Function	Cq	CqMean	CqStd	Quantity	Tm	RFU
H2	Sample 16	Channel1	FAM	UNKNOWN	39.831	39.831	0	0	79.394	18773
A3	Sample 17	Channel1	FAM	UNKNOWN	39.428	39.428	0	0	64.347	0
B3	Sample 18	Channel1	FAM	UNKNOWN	40.552	40.552	0	0	78.351	11817
C3	Sample 19	Channel1	FAM	UNKNOWN	35.064	35.064	0	0	80.177	15768
D3	Sample 20	Channel1	FAM	UNKNOWN	33.833	33.833	0	0	79.392	22012
E3	Sample 21	Channel1	FAM	UNKNOWN	29.511	29.511	0	0	79.554	21372
F3	Sample 22	Channel1	FAM	UNKNOWN	42.235	42.235	0	0	66.997	64
G3	Sample 23	Channel1	FAM	UNKNOWN	35.064	35.064	0	0	79.052	14979
H3	Sample 24	Channel1	FAM	UNKNOWN	43.534	43.534	0	0	65.319	14
A4	Sample 25	Channel1	FAM	UNKNOWN	42.363	42.363	0	0	64.546	123
B4	Sample 26	Channel1	FAM	UNKNOWN	36.025	36.025	0	0	78.991	21752
C4	Sample 27	Channel1	FAM	UNKNOWN	35.052	35.052	0	0	79.641	17298
D4	Sample 28	Channel1	FAM	UNKNOWN	36.103	36.103	0	0	78.505	12215
E4	Sample 29	Channel1	FAM	UNKNOWN	36.06	36.06	0	0	78.601	13855
F4	Sample 30	Channel1	FAM	UNKNOWN	43.304	43.304	0	0	65.147	23

*Cq: means cycle threshold, which is the cycle at which mass detection occurs.

*CqStd: means the cycle standard deviation threshold and is a standard deviation of the

fundamental Cq values.

*Tm means melting temperature, which is the temperature at which molecules are melted.

*RFU means relative fluorescent units, a unit of measurement for the intensity of quenching used in detection operations.

3.4 Statistical analysis

Every statistical analysis was conducted utilising GraphPad Prism version 9.0, developed by GraphPad Software in California, United States. The mean plus or minus the standard deviation (SD) or the median with the interquartile range (IQR) was utilised to represent continuous data. Conversely, categorical variables were represented in the form of frequencies and percentages. The Shapiro-Wilk test was implemented to ascertain the normality of the data. Given the deviation of the data from a normal distribution, comparisons between the groups were conducted utilising

non-parametric tests. The Mann-Whitney U test was utilised to compare the relative levels of miR-425 expression in the control and ill groups. The Kruskal-Wallis test was employed to facilitate a comparison of the relative levels of miR-425 expression among several distinct groups. Controls and patients with various types of breast cancer comprised these cohorts. After identifying significant differences between the groups using the Kruskal-Wallis test, post-hoc pairwise comparisons were conducted using Dunn's test with Bonferroni correction. Spearman's rank correlation was additionally employed to examine the relationship between age and relative miR-425 expression levels.

Conversely, the point-biserial correlation was employed to assess the correlation between residence, sex, and relative miR-425 expression levels. Every individual constituent underwent the computation of correlation coefficients (r) and p-values. Subsequently, a receiver operating characteristic (ROC) curve analysis was conducted to evaluate the diagnostic efficacy of miR-425 expression levels in distinguishing between healthy control subjects and individuals afflicted with diverse breast disorders. The area under the curve (AUC), sensitivity, specificity, and suitable cut-off values were calculated for each comparison.

Further computations were executed as well. The optimal cut-off values were determined by utilising the Youden index, which maximises the product of sensitivity and specificity. All experiments were performed utilising two-tailed testing, and statistical significance was defined as a p-value below 0.05. Considering the existence of multiple comparisons, the Bonferroni adjustment for post-hoc pairwise comparisons was implemented to modify the significance level.

3.4.1 Interpretation of the Results

The research investigation comprised a sample size of 10 controls and 20 cases. The analysts determined that the age difference between the two groups was not statistically significant (P = 0.840). Fifteen patients and seven controls resided in urban environments; the difference between the two groups was not deemed statistically significant (P = 0.435). Moreover, urban areas were home to the vast majority of the participants. Furthermore, treatment was administered to only three of the patients and not any of the controls; this distinction, however, failed to satisfy the requirements for statistical significance (P = 0.138).

The discrepancies in miR-425 expression levels between the 10 control participants and the 20 breast cancer patients are depicted in Figure (4.9). The median signifies the interquartile range (IQR) and is visually depicted as a horizontal line within the box. The minimum and maximum values the whiskers attain are 1.5 times the interquartile range (IQR) between the lowest and highest quartiles, respectively. When the relative miR-425 expression of the groups was compared using the Mann-Whitney U test, no statistically significant difference was found (p>0.05). The median relative miR-425 expression in the ill group was 1.05 (IQR: 0.50–1.72), whereas in the control group, it was 0.91 (IQR: 0.64–1.88).

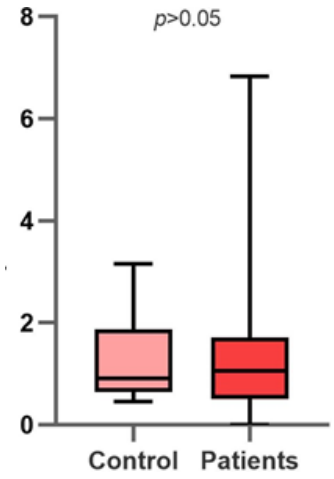

Figure 3.9. Illustrates the differences in miR-425 expression levels.

To gain a more comprehensive understanding of the situation, the Kruskal-Wallis test was employed to compare the relative levels of miR-425 expression among multiple groups comprising control subjects and patients afflicted with breast cancer disorders. In contrast to the control group, the relative median expression levels miR-425 were 1.34 (interquartile range: 0.50–1.96); 0.91 (interquartile range: 0.64–1.88).

The results of the Kruskal-Wallis test indicated that the relative expression of miR-425 varied significantly between groups ($p < 0.05$). No observable differences were identified between the control and patient groups that constituted the investigation. The results indicate that the severity of breast cancer may influence the expression of miR-425, as the disease is associated with a decreased level of miR-425. The median relative expression levels for the controls and the patients were 0.91 (interquartile range: 0.62–2.27), 0.89 (interquartile range: 0.66–1.31), and 1.12, respectively between 0.58 and 0.95 (interquartile range: 0.48 to 1.02 and 1.73, respectively).

The mean rankings for each subgroup were as follows: patients (17.10), controls (26.82), and patients (22.92). The Kruskal-Wallis test revealed, at a significance level of $p < 0.05$, that the relative levels of miR-425 expression did not differ significantly among the four categories. Based on the available data, obesity did not significantly affect the relative levels of miR-425 expression in either the control or ill groups. Furthermore, the levels of miR-425 expression were compared between individuals residing in urban and rural areas and between the control group and the ill group, using the Kruskal-Wallis test. A noteworthy disparity was observed between the median expression levels of the rural control group (1.04) and the urban control group (0.77): 1.56 (interquartile range: 1.16–1.86) versus 1.04 (interquartile range: 1.59–1.33).

The difference between the two values was 1.05 (interquartile range: 0.44–1.58). The Kruskal-Wallis test revealed that the relative levels of miR-425 expression did not differ significantly by residence among the four subgroups ($p>0.05$). This finding suggests no statistically significant difference in the relative levels of miR-425 expression between the control and patient groups, regardless of residential status (rural or urban).

A comparison of the relative expression levels of miR-425 in the following groups is depicted in Figure (4.10). Patients and members of the control group reside in rural and urban areas and the entire control group. The median signifies the interquartile range (IQR) and is visually depicted as a horizontal line within the box. The whiskers denote the minimum and maximum values that occur at intervals of 1.5 times the interquartile range (IQR) between the bottom and top quartiles. A significance level of * at $p<0.05$ and ** at $p<0.01$, respectively, is indicated.

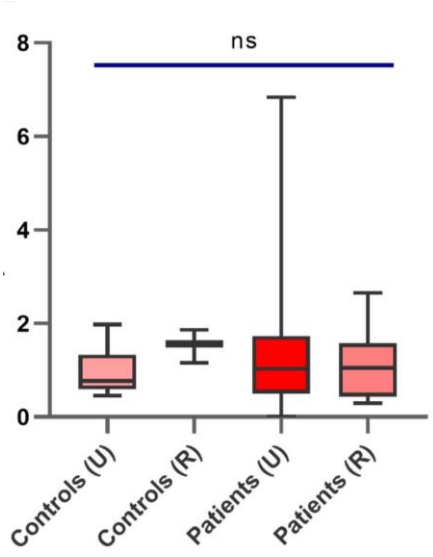

Figure 3.10 Box plot comparing the relative expression levels of miR-425

A correlation analysis assessed the relationship between relative levels of miR-425 expression and various characteristics, including age and residency. Utilising the Spearman rank correlation for the age variable. Based on the results, it was concluded that the relationships between the relative levels of miR-425 expression and each of the evaluated parameters were faint and insignificant. The correlation coefficient for age was r= 0.102 (p>0.05), suggesting moderate evidence supporting a positive association.

The scatter diagrams and correlation coefficients presented in Figure (4.11) illustrate the correlation between relative expression levels miR-425 and variables such as age and place of residence. Spearman's rank correlation coefficient was employed to assess age to determine the degree of association, while the point-biserial correlation coefficient was utilised to evaluate domicile. For each factor, correlation coefficients (r) and p-values are displayed.

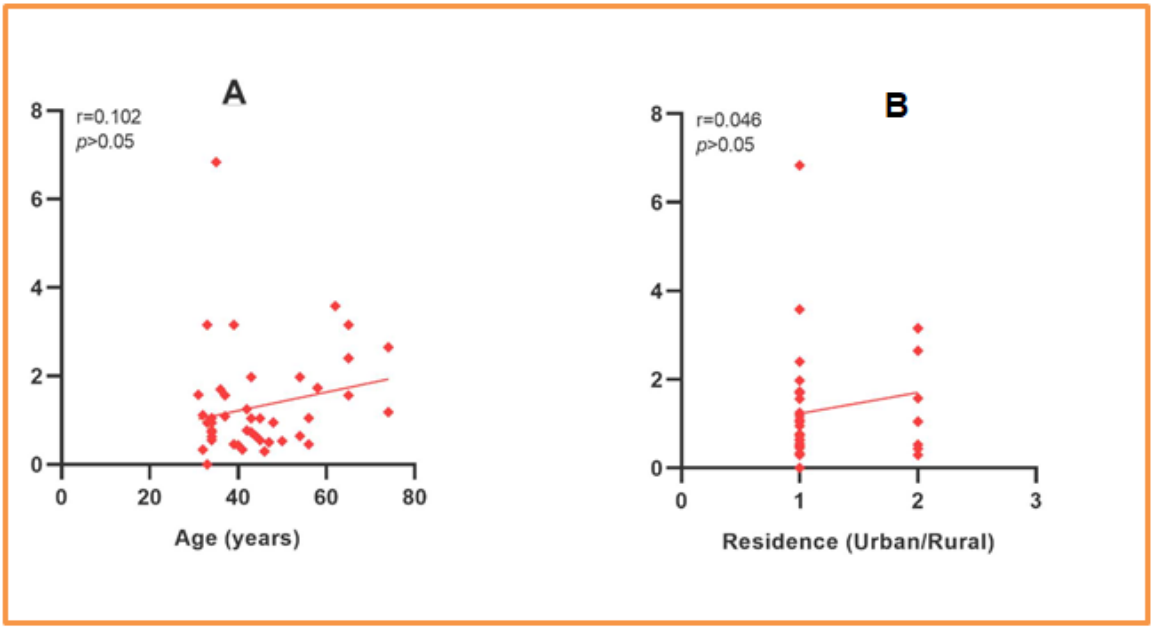

Figure 3.11 Displays scatter plots and correlation coefficients.

Curve analysis was performed to evaluate the diagnostic efficacy of miR-425 expression levels in terms of their capacity to distinguish between persons not diagnosed with breast cancer and those with a receiver operating characteristic (ROC). The control and patient groups were included in the calculations to find the area under the curve (AUC), sensitivity, specificity, and suitable cut-off values for each comparison (Table 4.8). An area under the curve (AUC) of 0.703 was obtained from the ROC curve study that compared the patients to the control group. At a cut-off value of >1.358, p>0.05, the sensitivity and specificity were 66.7% and 76.5%, respectively, with a 95% confidence interval between 11.9% and 98.3%.

The receiver operating characteristic (ROC) curves presented in Figure (4.12) illustrate the diagnostic capability of miR-425 expression levels in differentiating between control participants and breast cancer patients. For each comparison, the outcomes comprise the area under the curve (AUC), suitable cut-off values, sensitivity, and specificity. The dotted line denotes the reference line and has an area under the curve (AUC) value of 0.5.

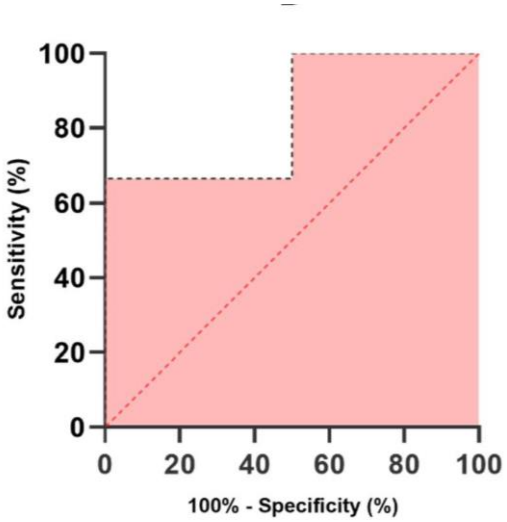

Figure 3.12 Depicts receiver operating characteristic (ROC) curves

Table 3.8. MiR-425 expression levels separate breast cancer patients from controls.

Control vs. Breast cancer		Sensitivity (%, 95% CI)	Specificity (%, 95% CI)	AUC	Cut-off	*P*
Control Cancer	vs.	66.7 (11.9 – 98.3)	76.5 (52.7 – 90.4)	0.569	>1.358	>0.05

3.5 Discussion

Based on the findings of this investigation, it was determined that microRNAs have the potential to be used as trustworthy biomarkers, which possess both predictive and prognostic relevance concerning breast cancer.

There are challenges associated with the early diagnosis of breast tumours (Cui, Chunmei, et , al 2022 , Cardoso, Fátima, et al. 2019) even though there are cancer treatment approaches that include both surgical and non-surgical procedures for breast cancer. A better treatment result is possible when the disease is detected earlier. It has been shown that microRNAs found in many bodily fluids have a strong link with the pathological aspects of cancer (Cui, Chunmei, et ,al 2020).

By comparing blood samples from twenty breast cancer patients and ten healthy persons, the purpose of the research was to investigate the function that microRNA molecules play in the diagnosis of breast cancer. It was discovered via the examination of the age distribution in both groups that those with breast cancer had an average age of fifty years, while healthy individuals had an average age of forty years. This discovery is consistent with the current body of research, which suggests that the incidence of breast cancer rises with age, especially beyond the age of 50 (Mahardhika, et ,al 2021). Examining the microRNA expression patterns using the procedures micRNA-16 and Micro 425 indicated significant variations between the two groups investigated. Within the framework of protocol micRNA-16, there were discernible differences in the cycle threshold (Cq) values between cancer samples and healthy controls. Cancer samples generally had lower Cq values, indicating greater levels of microRNA expression. Previous research has shown that breast cancer is associated with dysregulated microRNA expression (Aljofan, Mohamad, et , al 2019) , and our conclusion is consistent with that study.

On the other hand, the Cq values of cancer and healthy samples were shown to vary in a manner seen in procedure micRNA-425. However, there were significant changes in the degrees of fluorescence and melting temperatures, suggesting differences in the composition of microRNA between the two groups. It is important to note that the existence of metastasis in some cancer samples, as suggested by the BI-RADS result, may be a factor that contributes to the observed

diversity in microRNA expression patterns. These results emphasise the potential usefulness of microRNA molecules as biomarkers for breast cancer detection. They also highlight the need for additional exploration into these molecules' diagnostic value and clinical applicability.

The micRNA-16 and micRNA-425 have been shown to display both tumour suppressor and oncogenic behaviours across a wide range of cancer types, according to several studies published in the existing body of research (Xu, Jingjing, et al. 2019) . The results of our research indicate that the levels of micRNA-16 in the breast cancer group were much lower than those in the control group. This suggests that the micRNA-16 levels were downregulated in a manner comparable to that of a tumour suppressor.

There is a reduction in cell mobility, separation, and migration in breast cancer patients, shown by the high level of this miRNA type. This finding shows that the cell is more stable in these individuals, qualities that tend to inhibit (Hamamoto, Ryuji, et al. 2022) . The levels of micRNA-425 were lower in the sick group than in our research's control group. Previous research by (Loh, Hui-Yi, et al. 2019) has shown that micRNA-425 is a predictive biomarker with tumour suppressor capabilities in breast cancer. A drop in the expression level of micRNA-425, shown to have a statistically negative association with the number of breast cancer foci in our investigation and an increase in the number of tumour foci, were both proven to be multicentric. This was in addition to the findings of their study. Following these findings, during the process of planning breast-conserving surgery, it could be advantageous to take into consideration the possibility of a greater risk of multicentricity in patients who have low levels of micRNA-425. By taking this into account, the goal is to reduce the likelihood of local recurrences and to guarantee the complete eradication of tumours, hence reducing the likelihood that patients will have residual lesions.

The results of our research indicated that the expression levels of micRNA-425 were higher in the patient group than in the control group. This was the case in some of the patients. micRNA-425 readings were greater in patients with a negative E-cadherin test and those with a significant number of lymph nodes with metastatic disease. It seems from this that an increase in micRNA-425 might potentially lead to an increase in the number of metastatic lymph nodes and the spread of the tumour by having a detrimental effect on the stability of the cells. These findings consistently enhance the tumour's capacity to grow and spread. Even though the literature has shown that Mic-425 has an abnormal expression pattern in a variety of malignancies, the mechanism of action of this protein has not yet been completely elucidated (Gulyaeva, Lyudmila F et , al 2016)

The micRNA-425 expression was shown to be related to chemotherapeutic resistance in breast cancer, according to the findings of certain research. The results of our research indicate that Mic-425 has the potential to be a biomarker that is linked with a bad prognosis. High levels of micRNA-425 may indicate a more aggressive tumour. As a result, adding this information into the consideration of adjuvant therapy after surgery might potentially help treatment planning that is more informed and focused.

References

1. DeSantis, Carol E., et al. "Breast cancer statistics, 2019." *CA: a cancer journal for clinicians* 69.6 (2019): 438-451.
2. Rej, Rohan Kalyan, Joyeeta Roy, and Srinivasa Rao Allu. "Therapies for the Treatment of Advanced/Metastatic Estrogen Receptor-Positive Breast Cancer: Current Situation and Future Directions." *Cancers* 16.3 (2024): 552.
3. Han, Yiqun, Jiayu Wang, and Binghe Xu. "Clinicopathological characteristics and prognosis of breast cancer with special histological types: a surveillance, epidemiology, and results database analysis." *The Breast* 54 (2020): 114-120.

   Behairy, Mahmoud, Samia Mohamed Gabal, and Mohamed Sherif Negm. "Breast cancer human epidermal growth factor receptor 2 mRNA molecular testing compared to

immunohistochemistry with correlation to neoadjuvant therapy response." *Open Access Macedonian Journal of Medical Sciences* 10.A (2022): 352-356.

4. Sparano, Joseph A., et al. "Clinical outcomes in early breast cancer with a high 21-gene recurrence score of 26 to 100 assigned to adjuvant chemotherapy plus endocrine therapy: a secondary analysis of the TAILORx randomized clinical trial." *JAMA oncology* 6.3 (2020): 367-374.
5. Turkki, Riku, et al. "Breast cancer outcome prediction with tumour tissue images and machine learning." *Breast cancer research and treatment* 177 (2019): 41-52.
6. Annese, Tiziana, et al. "microRNAs biogenesis, functions and role in tumor angiogenesis." *Frontiers in oncology* 10 (2020): 581007.
7. Hussen, Bashdar Mahmud, et al. "MicroRNA: A signature for cancer progression." *Biomedicine & Pharmacotherapy* 138 (2021): 111528.
8. Li, Lu, et al. "Widespread microRNA degradation elements in target mRNAs can assist the encoded proteins." *Genes & development* 35.23-24 (2021): 1595-1609.
9. Shafabakhsh, Rana, et al. "Association between microRNAs expression and signaling pathways of inflammatory markers in diabetic retinopathy." *Journal of cellular physiology* 234.6 (2019): 7781-7787.
10. Abadi, Mohammad Hassan Jafari Najaf, et al. "CFIm25 and alternative polyadenylation: Conflicting roles in cancer." *Cancer letters* 459 (2019): 112-121.